Neurobiology of Disease

Targeted Disruption of Na^+/Ca^{2+} Exchanger 3 (NCX3) Gene Leads to a Worsening of Ischemic Brain Damage

Pasquale Molinaro,[1]* Ornella Cuomo,[1]* Giuseppe Pignataro,[1]* Francesca Boscia,[1]* Rossana Sirabella,[1] Anna Pannaccione,[1] Agnese Secondo,[1] Antonella Scorziello,[1] Annagrazia Adornetto,[1] Rosaria Gala,[1] Davide Viggiano,[1] Sophie Sokolow,[2] Andre Herchuelz,[2] Stèphane Schurmans,[3] Gianfranco Di Renzo,[1] and Lucio Annunziato[1]

[1]Division of Pharmacology, Department of Neuroscience, School of Medicine, "Federico II" University of Naples, 80131 Naples, Italy, [2]Laboratory of Pharmacology and Therapeutics, and [3]Institut de Recherches en Biologie Humaine et Moléculaire-Institut de Biologie et de Médecine Moléculaires, Université Libre de Bruxelles, 6041 Gosselies, Belgium

Na^+/Ca^{2+} exchanger 3 (NCX3), one of the three isoforms of the NCX family, is highly expressed in the brain and is involved in the maintenance of intracellular Na^+ and Ca^{2+} homeostasis. Interestingly, whereas the function of NCX3 under physiological conditions has been determined, its role under anoxia is still unknown. To assess NCX3 role in cerebral ischemia, we exposed ncx3−/− mice to transient middle cerebral artery occlusion followed by reperfusion. In addition, to evaluate the effect of ncx3 ablation on neuronal survival, organotypic hippocampal cultures and primary cortical neurons from ncx3−/− mice were subjected to oxygen glucose deprivation (OGD) plus reoxygenation. Here we report that ncx3 gene suppression leads to a worsening of brain damage after focal ischemia and to a massive neuronal death in all the hippocampal fields of organotypic cultures as well as in cortical neurons from ncx3−/− mice exposed to OGD plus reoxygenation. In addition, in ncx3−/− cortical neurons exposed to hypoxia, NCX currents, recorded in the reverse mode of operation, were significantly lower than those detected in ncx3+/+. From these results, NCX3 protein emerges as a new molecular target that may have a potential therapeutic value in modulating cerebral ischemia.

Key words: **NCX; MCAO; cerebral ischemia; sodium calcium exchanger; OGD; organotypic hippocampal cultures**

Introduction

The Na^+/Ca^{2+} exchanger (NCX) (Philipson and Nicoll, 2000; Annunziato et al., 2004) is a nine-transmembrane domain protein that couples, in a bidirectional way, the influx/efflux of Ca^{2+} to the efflux/influx of Na^+ ions. Interestingly, whereas the function of NCX under physiological conditions has been determined, its function under anoxic conditions is still unknown. In fact, in the early phase of neuronal anoxic insult, the initial blockade of Na^+-K^+ ATPase increases $[Na^+]_i$ (Amoroso et al., 1997; Jones et al., 2006), which, in turn, elicits a profound Ca^{2+} entry through the activation of the NCX reverse mode of operation. Although the reverse mode of operation elicits an increase in $[Ca^{2+}]_i$, its effect could be beneficial for neurons, because it contributes to a decrease in $[Na^+]_i$ overload, thus preventing cell swelling and death. Conversely, in the later phase of neuronal anoxia, when $[Ca^{2+}]_i$ overload takes place, NCX forward mode of operation contributes to the lowering of $[Ca^{2+}]_i$, thus protecting neurons from $[Ca^{2+}]_i$-induced neurotoxicity (Amoroso et al., 1997). Another element of complexity in the role played by NCX in the events leading to anoxic neurodegeneration is the existence of three different gene products, NCX1, NCX2, and NCX3 (Philipson and Nicoll, 2000; Annunziato et al., 2004), which indeed display different expression patterns in the brain under physiological (Papa et al., 2003) and pathophysiological (Boscia et al., 2006b) conditions. Particularly, in the ischemic core region, NCX1, NCX2, and NCX3 mRNAs and proteins are downregulated in those areas surviving the ischemic insult (Pignataro et al., 2004b; Boscia et al., 2006b). In contrast, in the periischemic area, NCX2 is downregulated, whereas NCX3 is upregulated (Boscia et al., 2006b). This upregulation could be interpreted as a compensatory mechanism that counterbalances NCX2 reduced activity, thus alleviating the dysregulation of $[Na^+]_i$ and $[Ca^{2+}]_i$ homeostasis.

In addition, these three gene products display differential sensitivity to intracellular ATP levels (Linck et al., 1998). In fact, whereas ATP is required for NCX1 and NCX2 activity, NCX3 is able to operate in the absence of this nucleotide (Secondo et al., 2007). Indeed, NCX3 independence of ATP is suggestive of its evolutionary role in counterbalancing ATP depletion during brain ischemia. Here, we propose NCX3 protein as a distress signal able to modulate intraneuronal Na^+ and Ca^{2+} homeostasis whenever neurons undergo severe anoxia.

To test this hypothesis, we assessed NCX3 role in cerebral

Received July 6, 2007; revised Dec. 5, 2007; accepted Dec. 6, 2007.

This work was supported by grants from COFIN 2006, Regione Campania GEAR, Ricerca Finalizzata Ministero della Salute Legge 502/92 "Geni Vulnerabiltà e di Riparazione DNA," Legge 5/2003, and by "Ministero Affari Esteri, Direzione Generale per la Promozione e la Cooperazione Culturale Fondi Italia-Cina Legge 401/1990 2007" (all to L.A.). We thank Prof. K. D. Philipson and Dr. D. A. Nicoll (University of California, Los Angeles) for providing us anti-NCX3 antibody, Drs. Guido Laccarino and Alfonso Campanile for helping us with measuring MABP, Dr. Paola Merolla for the editorial revision, and Vincenzo Grillo and Carmine Capitale for the technical support.

*P.M., O.C., G.P., and F.B. contributed equally to this work.

Correspondence should be addressed to Dr. Lucio Annunziato, Division of Pharmacology, Department of Neuroscience, School of Medicine, "Federico II" University of Naples, Via Pansini 5, 80131 Naples, Italy. E-mail: lannunzi@unina.it.

S. Sokolow's present address: University of California, Los Angeles School of Nursing, Los Angeles, CA 90095.

DOI:10.1523/JNEUROSCI.4671-07.2008

 0270-6474/08/281179-06$15.00/0

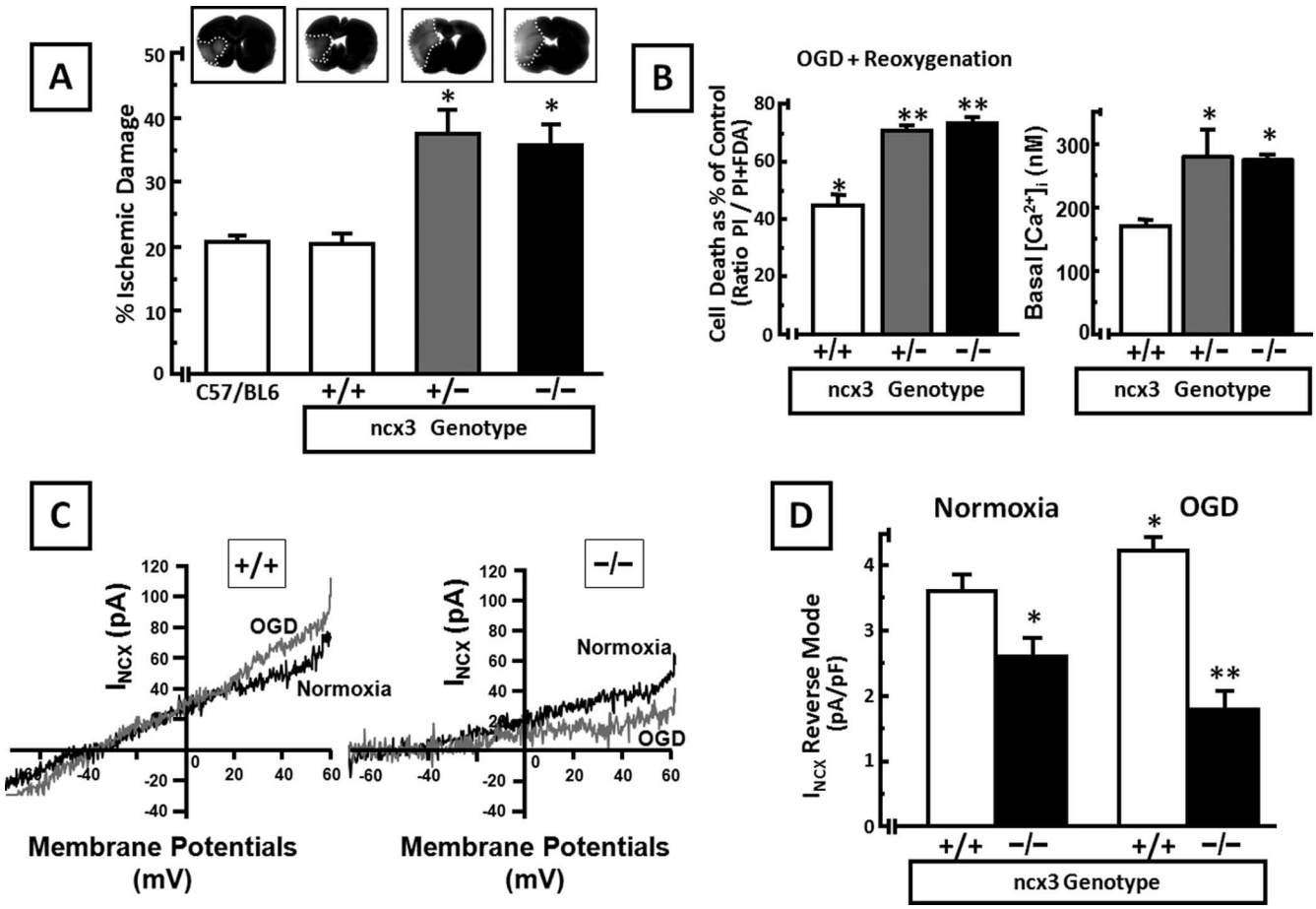

Figure 1. Effect of ncx3 ablation on brain ischemia, neuronal survival under hypoxic conditions, $[Ca^{2+}]_i$, and I_{NCX}. ***A***, Effect of ncx3 knocking-out on infarct volume in C57BL/6 wild-type and congenic ncx3+/+, ncx3+/−, and ncx3−/− mice, respectively, subjected to tMCAo. Each column represents the mean ± SEM of the percentage of the infarct volume compared with the ipsilateral hemisphere. Ischemic mice were killed 24 h after tMCAo. *$p < 0.05$ versus C57BL/6 wild-type and congenic ncx3+/+ ischemic mice. $n = 9–18$ animals for each column. A representative brain slice from each ischemic experimental group is shown on the top of each column. ***B***, Effect of NCX3 knock-out on survival of cortical neurons exposed to OGD plus reoxygenation. Left, Cell death quantification was performed by PI and fluorescein dyes in 7–10 DIV embryonic cortical neurons obtained from ncx3+/+, ncx3+/−, and ncx3−/− mice exposed to 3 h of OGD followed by 21 h of reoxygenation or to 24 h of normoxia. At the end of the experiments, cells were stained with PI and fluorescein, and images were acquired as reported in Materials and Methods. The data are reported as percentage of cell death occurring in each group compared with their respective normoxic cells. In normoxic conditions, ncx3+/+, ncx3+/−, and ncx3−/− cortical neurons showed similar levels of cell death (~15%). *$p < 0.05$ versus respective normoxic neurons ; **$p < 0.05$ versus respective normoxic neurons and versus ncx3+/+ group. Each bar represents the mean ± SEM of three different experimental values studied in three independent experimental sessions. Right, The bar graph represents basal fura-2 AM-detected $[Ca^{2+}]_i$ in 7–10 DIV cortical neurons from ncx3+/+, ncx3+/−, and ncx3−/− mice. *$p < 0.05$ versus ncx3+/+. fura-2 AM fluorescence intensity was measured every 3 s for 5 min. The values obtained in this interval were averaged for each cortical neuron. Each bar represents the mean ± SEM of at least 70 cortical neurons in three different experimental sessions. ***C***, ***D***, Effect of ncx3 knocking-out on I_{NCX} recorded in the reverse mode of operation in 7–10 DIV embryonic cortical neurons. ***C***, I_{NCX} superimposed traces recorded from ncx3+/+ (left) and ncx3−/− (right) cortical neurons under normoxic conditions (black traces) and after 3 h of OGD (gray traces). ***D***, I_{NCX} quantification expressed as pA/pF, in ncx3+/+ and ncx3−/− cortical neurons in control conditions and after 3 h of OGD. The values are expressed as mean ± SEM of current densities recorded from 20 cells in each experimental group obtained from three independent experimental sessions. *$p < 0.05$ versus ncx3+/+ normoxic neurons ; **$p < 0.05$ versus all the other experimental groups.

ischemia by exposing ncx3−/− mice generated by our research group (Sokolow et al., 2004) to transient middle cerebral artery occlusion (tMCAo). Moreover, to evaluate the effects of ncx3 ablation on neuronal survival, organotypic hippocampal cultures and primary cortical neurons from ncx3−/− mice were subjected to oxygen glucose deprivation (OGD) plus reoxygenation. Finally, NCX currents (I_{NCX}), in the reverse mode of operation, were evaluated by means of the patch-clamp technique in ncx3−/− cortical neurons exposed to hypoxia.

Materials and Methods

Experimental groups. C57BL/6 wild-type, ncx3+/+, ncx3+/−, and ncx3−/− mice aged between 6 and 8 weeks and weighing 27–30 g were housed under diurnal lighting conditions. Experiments were performed according to the international guidelines for animal research and approved by the Animal Care Committee of "Federico II" University of Naples, Italy.

tMCAo model. Mice were subjected to tMCAo as described previously (Longa et al., 1989). A 5-0 nylon filament was inserted through the external carotid artery stump and advanced into the right internal carotid artery until it blocked the origin of the MCA. After 60 min of MCA occlusion, the filament was withdrawn to restore blood flow. Body temperature was monitored throughout the entire duration of the surgical procedure and maintained at 37.5°C with a thermostatic blanket.

Monitoring of arterial blood pressure and cerebral blood flow. Arterial blood pressure was measured with a catheter that was first inserted into the common carotid artery, then connected to solid-state pressure transducers (Power lab system; ADInstruments, Castle Hill, New South Wales, Australia), and lastly analyzed by CHART Windows software. No difference in diastolic and systolic arterial blood pressure was detected in the two experimental groups of ncx3+/+ and ncx3−/− mice. Cerebral

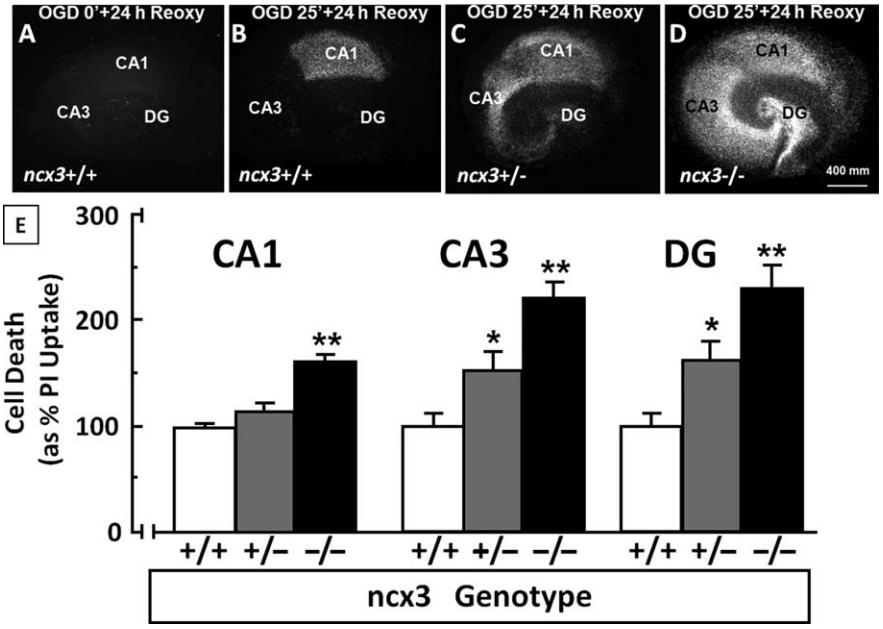

Figure 2. Neuronal survival in CA1, CA3, and DG subregions of OHSCs from ncx3+/+, ncx3+/−, and ncx3−/− mice exposed to OGD plus reoxygenation (Reoxy). ***A***, PI fluorescence in ncx3+/+ OHSCs after their exposure to 25 min of normoxia followed by 24 h of normoxic and normoglycemic conditions. ***B–D***, PI fluorescence in OHSCs obtained from congenic ncx3+/+ (***B***), ncx3+/− (***C***), and ncx3−/− (***D***) mice, exposed to 25 min of OGD followed by 24 h of reoxygenation. ***E***, Quantification of the cell damage in selected hippocampal subregions, CA1, CA3, and DG, from congenic ncx3+/+, ncx3+/−, and ncx3−/− mice evaluated by densitometric analysis of PI fluorescence. PI fluorescence intensity recorded in each hippocampal subfield was normalized to that recorded in the respective subregion of OHSCs from congenic ncx3+/+ mice exposed to 25 min of OGD plus 24 h of reoxygenation, which was considered as 100%. All the values of the experimental groups were expressed as percentage of PI fluorescence. Each data point is the mean ± SEM of the data obtained from 20–24 OHSCs in three separate experiments. Scale bar in ***A–D***, 400 μm. *$p < 0.05$ versus congenic ncx3+/+ OHSCs exposed to OGD/reoxygenation; **$p < 0.05$ versus ncx3+/+ and ncx3+/− OHSCs exposed to OGD/reoxygenation.

blood flow (CBF) was monitored in the cerebral cortex ipsilateral to the occluded MCA with a laser-Doppler flowmeter (Periflux system, 5000). Once a stable CBF signal was obtained, the MCA was occluded. CBF was monitored throughout the 1 h occlusion period and the first 30 min of reperfusion. Only those mice that reached at least 70% of CBF reduction after MCAo were included in the experimental groups (Pignataro et al., 2007).

Evaluation of the ischemic volume. Ischemic volume was evaluated by 2,3,5-triphenyl tetrazolium chloride staining 24 h after ischemia induction. The infarct area was calculated with image analysis software (Image-Pro Plus) (Pignataro et al., 2004a). To avoid a possible overestimation of the infarct volume as a result of the presence of edema, the total infarct volume was expressed as percentage of the volume of the hemisphere ipsilateral to the lesion (Pignataro et al., 2004a). Ischemic volumes were evaluated in a blind manner.

Primary cortical neurons and hippocampal organotypic slice cultures. Cortical neurons were prepared from brains of 14-d-old mouse embryos, plated on coverslips, and cultured in MEM/F12 (Invitrogen, Milan, Italy) containing glucose, 5% of deactivated fetal bovine serum, and 5% horse serum (Invitrogen), glutamine (2 mM), penicillin (50 U/ml), and streptomycin (50 μg/ml). Cytosine-β-D-arabino-furanoside (10 μM) was added within 48 h of plating to prevent the growth of non-neuronal cells. Neurons were cultured at 37°C in a humidified 5% CO_2 atmosphere and used after 7–10 d *in vitro* (DIV) (Scorziello et al., 2007).

Organotypic hippocampal slice cultures (OHSCs) were prepared as previously described (Boscia et al., 2006a). Briefly, 400-μm-thick coronal brain slices from postnatal day 5 (P5)–P7 ncx3+/+, ncx3+/−, and ncx3−/− mouse pups were used. To increase the reproducibility of the data, two consecutive slices from the two hippocampi of the same animal were always dissected at the same level in all the experimental groups. Slices were grown on semipermeable filter inserts (Millipore, Billerica, MA) in six-well plates containing culture medium (50% minimum essential medium, 25% HBSS, 25% heat-inactivated horse serum, 5 mg/ml glucose, 1 mM glutamine, 1% Fungizone). The culture period was 14 d. Hypoxic conditions were induced by exposing hippocampal cultures and cortical neurons to oxygen- and glucose free-medium in a humidified atmosphere containing 95% nitrogen and 5% CO_2 (Boscia et al., 2006a; Scorziello et al., 2007). After 25 min of OGD followed by 24 h of reoxygenation, cell injury of organotypic slices was assessed using the fluorescent dye propidium iodide (PI) (Invitrogen). Its uptake was recorded by a digital camera (Media Cybernetics, Silver Springs, MD) mounted on a Nikon Eclipse 400 fluorescence microscope (Nikon Instruments, Florence, Italy). For densitometric measurements, the digital photos were analyzed with the Image Pro-Plus software (Media Cybernetics), after freehand outlining of the CA1, CA3, and dentate gyrus (DG) neuronal layers was performed as previously described (Boscia et al., 2006a). Densitometric data were obtained by an integrated algorithm that considers the mean of optical density (Boscia et al., 2006a). In primary cortical neurons, cell injury was assessed after 3 h of OGD followed by 21 h of reoxygenation. PI- (7 μM) and fluorescein diacetate (FDA; 36 μM)-positive cells were counted in three representative high-power fields of independent cultures, and cell death was determined by the ratio of the number of PI-positive cells/PI+FDA-positive cells.

$[Ca^{2+}]_i$ imaging. $[Ca^{2+}]_i$ was measured in normoxic conditions by fura-2 AM single-cell computer-assisted video imaging (Secondo et al., 2007).

Electrophysiology. I_{NCX} was recorded from primary ncx3+/+ and ncx3−/− cortical neurons by the patch-clamp technique in whole-cell configuration. Currents were filtered at 5 kHz and digitized using a Digidata 1322A interface (Molecular Devices, Sunnyvale, CA). Data were acquired and analyzed using the pClamp software (version 9.0; Molecular Devices). Briefly, starting from a holding potential of −60 mV to a short-step depolarization at +60 mV (60 ms), the I_{NCX} were recorded (He et al., 2003). Then, a descending voltage ramp from +60 mV to −120 mV was applied, and the recorded current was used to plot the current–voltage (*I–V*) relation curve. The magnitudes of I_{NCX} were measured at the end of +60 mV (reverse mode) and at the end of −120 mV (forward mode). Next, as Ni^{2+} blocks I_{NCX}, $NiCl_2$ (5 mM) was routinely added to measure the NCX-independent currents. The Ni^{2+}-insensitive components were subtracted from total currents to isolate I_{NCX} (He et al., 2003). Cortical neurons were perfused with external Ringer solution containing the following (in mM): 126 NaCl, 1.2 $NaHPO_4$, 2.4 KCl, 2.4 $CaCl_2$, 1.2 $MgCl_2$, 10 glucose, and 18 $NaHCO_3$, pH 7.4. Tetraethylammonium (TEA; 20 mM), 50 nM tetrodotoxin (TTX), and 10 μM nimodipine were added to Ringer solution to block TEA-sensitive K^+, TTX-sensitive Na^+, and L-type Ca^{2+} currents, respectively. The dialyzing pipette solution contained the following (in mM): 100 K-gluconate, 10 TEA, 20 NaCl, 1 Mg-ATP, 0.1 $CaCl_2$, 2 $MgCl_2$, 0.75 EGTA, and 10 HEPES, adjusted to pH 7.2 with $Cs(OH)_2$. Possible changes in cell size occurring after specific treatments were calculated by monitoring the capacitance of each cell membrane, which is directly related to membrane surface area, and by expressing the current amplitude data as current densities (pA/pF). Capacitive currents were estimated from the decay of capacitative transient induced by 5 mV depolarizing pulses from a holding potential of −80 mV and acquired at a sampling rate of 50 kHz. The capacitance of the membrane was calculated according to the following equation: $C_m = \tau_c \times I_o/\Delta E_m(1 - I_\infty/I_o)$, where C_m is membrane capacitance, τ_c is the time constant of the membrane capacitance, I_o is the

maximum capacitance current value, ΔE_m is the amplitude of the voltage step, and I_∞ is the amplitude of the steady-state current.

Reverse transcription and real-time PCR. For reverse transcription, 4.0 μg of each RNA extract from nonischemic temporoparietal cortex and hippocampus was digested with DNase and reverse transcribed by SuperScript III (Invitrogen), according to Invitrogen protocol. The following sequences of primers were used: NCX1-forward, 5′-CCGTGACTGCCGTTGTGTT-3′; NCX1-reverse, 5′-GCCTATAGACGCATCTGCATACTG-3′; NCX2-forward, 5′-AGTGGATGATGAAGAGTATGAGAAGAAG-3′; NCX2-reverse, 5′-TTGGTTGAGTAGCAGAGCTGAGA-3′; NCX3-forward, 5′-CCTCTGTGCCAGATACATTTGC-3′; NCX3-reverse, 5′-CCAAACCAATACCCAGGAAGAC-3′; hypoxanthine-guanine phosphoribosyl transferase (HGPRT)-forward, 5′-TCCATTCCTATGACTGTAGATTTTATCAG-3′; HGPRT-reverse, 5′-AACTTTTATGTCCCCCGTTGACT-3′.

Protein expression analysis. Whole-cell protein extracts from dissected areas and embryonic cortical neurons of ncx3+/+, ncx3+/−, and ncx3−/− mice were obtained and processed as previously described (Secondo et al., 2007). Nitrocellulose membranes were incubated with anti-NCX1 antibody (rabbit polyclonal; Swant, Bellinzona, Switzerland; 1:1000 dilution), anti-NCX2 antibody (rabbit polyclonal; Alpha Diagnostics International, San Antonio, TX; 1:1000 dilution), anti-NCX3 antibody (rabbit polyclonal; 1:2000; kindly provided by K. D. Philipson and D. Nicoll, University of California, Los Angeles, CA) and anti-plasma membrane Ca^{2+} ATPase (PMCA) antibody (mouse monoclonal; Affinity BioReagents, Golden, CO; 1:1000 dilution). These nitrocellulose membranes were first washed with 0.1% Tween 20 and then incubated with the corresponding secondary antibodies for 1 h (GE Healthcare, Little Chalfont, UK). Immunoreactive bands were detected with the ECL (GE Healthcare). The optical density of the bands (normalized with β-actin) (Sigma, St. Louis, MO) was determined by Chemi-Doc Imaging System (Bio-Rad, Segrate, Italy).

Statistical analysis. Values are expressed as means ± SEM, and statistical analysis was performed with two-way ANOVA, followed by Newman–Keuls test. Statistical significance was accepted at the 95% confidence level ($p < 0.05$).

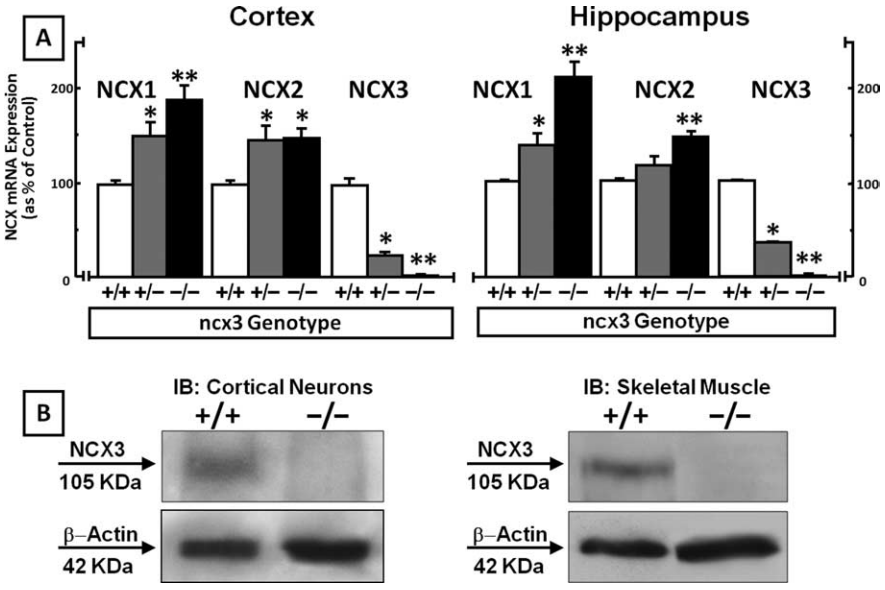

Figure 3. ***A***, Real-time PCR of NCX1, NCX2, and NCX3 mRNA expression in cortex and hippocampus from ncx3+/+, ncx3+/−, and ncx3−/− mice. Data were normalized on the basis of HGPRT levels and expressed as percentage of the respective ncx3+/+ control group, taken as 100%. Values represent means ± SEM ($n = 4$). *$p < 0.05$ versus each respective ncx3+/+ group; **$p < 0.05$ versus their respective ncx3+/+ and ncx3+/− groups. ***B***, Immunoblot (IB) of NCX3 and β-actin expression in 7–10 DIV embryonic cortical neurons (left) and skeletal muscle (right) from ncx3+/+ and ncx3−/− mice.

Results

Effect of ncx3 knocking-out on infarct volume in ncx3+/+, ncx3+/−, and ncx3−/− mice subjected to tMCAo and on survival in ncx3+/+, ncx3+/−, and ncx3−/− cortical neurons exposed to OGD plus reoxygenation

Examination of large cerebral vessels of the ventral brain side did not show anatomical differences in the circle of Willis among ncx3+/+, ncx3+/−, and ncx3−/− mice. Similarly, cortical and striatal capillary densities did not show significant variations in the two experimental groups (see supplemental material, available at www.jneurosci.org). ncx3 knocking-out dramatically increased the extent of the ischemic lesion in both ncx3−/− and ncx3+/− mice subjected to tMCAo compared with both wild-type C57BL/6 and congenic ncx3+/+ mice (Fig. 1*A*). The enlargement of the ischemic core in these genetically modified mice was particularly evident in the more peripheral temporoparietal cortex. ncx3+/− and ncx3−/− cortical neurons exposed to 3 h of OGD followed by 21 h of reoxygenation displayed a significant increase in cell death compared with ncx3+/+ group (Fig. 1*B*, left graph). Interestingly, basal $[Ca^{2+}]_i$ detected by single-cell fura-2 AM imaging was significantly higher in ncx3+/− and ncx3−/− cortical neurons than in ncx3+/+ cells (Fig. 1*B*, right graph).

Effect of ncx3 knocking-out on I_{NCX} in the reverse mode of operation in cortical neurons

In normoxic conditions, I_{NCX}, recorded in the reverse mode of operation by the whole-cell patch-clamp technique, was significantly lower in ncx3−/− primary cortical neurons than in ncx3+/+. More interestingly, when ncx3−/− primary cortical neurons were exposed to OGD, I_{NCX}, recorded in the reverse mode of operation, was lower than that observed in ncx3+/+ neurons (Fig. 1*C–D*).

Neuronal survival in CA1, CA3, and DG subregions of OHSCs from ncx3+/+, ncx3+/−, and ncx3−/− mice exposed to hypoxia plus reoxygenation

OGD followed by reoxygenation reduced cellular survival, as revealed by the increase in PI uptake in CA1, CA3, and DG hippocampal subregions from ncx3−/− mice compared with ncx3+/+ mice (Fig. 2*A–D*). Whereas in CA3 and DG fields, neuronal survival decreased by 60%, it increased by 130% in organotypic cultures obtained either from ncx3+/− or from ncx3−/− mice compared with congenic ncx3+/+ mice (Fig. 2*E*). In CA1 region of ncx3−/− mice, neurodegeneration was 60% higher than in the corresponding region of congenic ncx3+/+ animals (Fig. 2*E*). No difference in densitometric measurements of PI uptake was observed in OHSCs either from congenic ncx3+/+ mice (Fig. 2*A*) or from ncx3+/−, ncx3−/− mice under control conditions (data not shown).

Effect of ncx3 disruption on NCX1, NCX2, and NCX3 transcript expression in cortex and hippocampus

In the cortex and in the hippocampus of ncx3−/− and ncx3+/− mice, NCX1 and NCX2 transcript levels were significantly higher

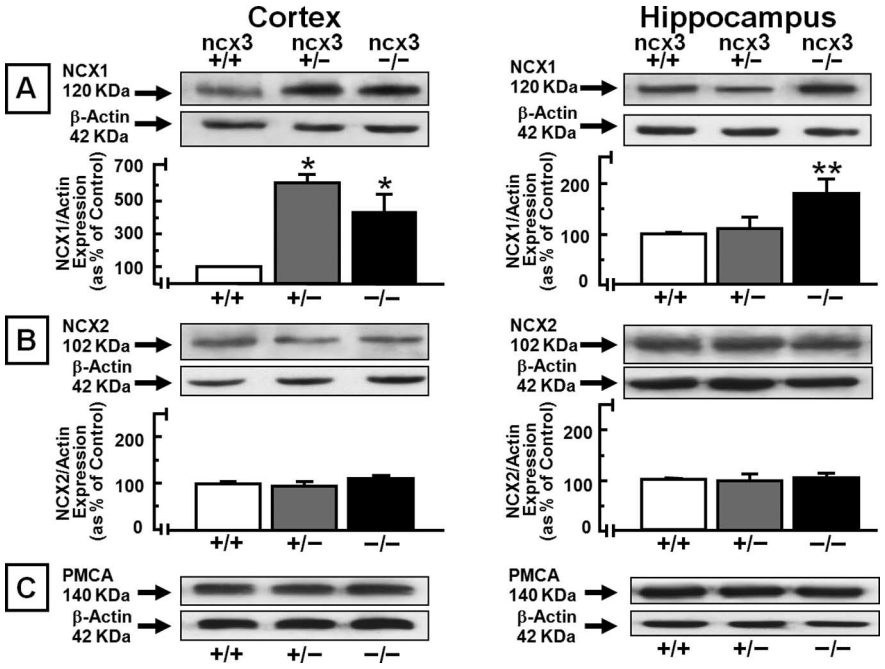

Figure 4. Immunoblot analysis of NCX1 (***A***), NCX2 (***B***), and PMCA (***C***) protein expression in cortex and hippocampus from ncx3+/+, ncx3+/−, and ncx3−/− mice. Data were normalized on the basis of β-actin levels and expressed as percentage of the respective ncx3+/+ control group, taken as 100%. Values represent means ± SEM ($n = 3–4$). *$p < 0.05$ versus ncx3+/+; **$p < 0.05$ versus ncx3+/+ and ncx3+/− groups.

than those in congenic ncx3+/+ mice, whereas in ncx3−/− mice, NCX3 mRNA was undetectable (Fig. 3*A*).

Effect of ncx3 disruption on NCX1, NCX2, and PMCA protein expression in cortex and hippocampus

In cortical neurons and skeletal muscle from ncx3−/− mice, the band corresponding to NCX3 protein was not present (Fig. 3*B*). In the cortex of ncx3−/− and ncx3+/− mice, NCX1 protein levels were significantly upregulated compared with those of congenic ncx3+/+ mice (Fig. 4*A*), whereas NCX2 protein levels were not modified (Fig. 4*B*). In the hippocampus, NCX1 was upregulated only in the ncx3−/− group (Fig. 4*A*). Protein levels of PMCA, a plasma membrane pump that cooperates with NCX in the maintenance of Ca^{2+} homeostasis, did not change in all the brain regions examined (Fig. 4*C*).

Discussion

The results of the present study demonstrate that ncx3 gene disruption renders the brain more susceptible to the ischemic insults induced by the tMCAo. This indicates that in ncx3+/+ mice, NCX3 protein attenuates the development of ischemic brain injury in those cerebral territories supplied by the MCA. The pivotal role played by NCX3 during ischemia is strongly supported *in vitro* (1) by the elevated basal levels of $[Ca^{2+}]_i$ observed in ncx3−/− and ncx3+/− cortical neurons compared with ncx3+/+ cells and (2) by the enhanced vulnerability of primary cortical neurons and hippocampal subregions CA1, CA3, and DG from ncx3−/− mice exposed to OGD followed by reoxygenation. Intriguingly, the more severe cell death observed in the CA3 and DG subregions compared with CA1 after ncx3 deletion might be attributable to the removal of this isoform in those hippocampal subregions, where it is more intensely expressed (Papa et al., 2003). Unlike NCX1 and NCX2, the peculiar capability of NCX3 to maintain $[Ca^{2+}]_i$ homeostasis even when ATP levels are reduced significantly highlights its major role in neuronal preservation during hypoxic conditions (Secondo et al., 2007). Consistently, we found that the compensatory upregulation of NCX1 in the cerebral cortex of ncx3−/− mice was insufficient to counterbalance the detrimental effects of ncx3 gene disruption on Ca^{2+} and Na^+ homeostasis during ischemia because of the impaired activity of NCX1 resulting from ATP depletion.

Interestingly, NCX3 silencing by RNA interference increases cerebellar granule neurons' vulnerability to Ca^{2+} overload and excitotoxicity (Bano et al., 2005), and it renders clonal cells stably transfected with NCX3 extremely vulnerable to chemical hypoxia (Secondo et al., 2007). Furthermore, NCX3 mRNA and protein downregulation, induced by the overexpression of DREAM (downstream regulatory element antagonist modulator), increases the mortality rate of cerebellar granule cells (Gomez-Villafuertes et al., 2005). In addition, ischemic rats treated with NCX3 antisense displayed a remarkable broadening of the infarct volume (Pignataro et al., 2004b). In agreement with this vicarious function proposed for NCX3, our recent *in vivo* experiments, entailing the induction of permanent MCAo in rats, have demonstrated that NCX3 mRNA is upregulated 24 h after the injury in brain regions belonging to the periinfarct area (Boscia et al., 2006b). This NCX3 upregulation, as opposed to NCX2 downregulation, has been interpreted as a compensatory mechanism that counterbalances the reduced activity of NCX2 protein, thus counteracting the dysregulation of $[Ca^{2+}]_i$ homeostasis in the surviving neurons of the penumbra zone (Boscia et al., 2006b).

In regard to the hypothetical mode of operation of NCX3 during stroke, it should be underlined that the region of maximum $[Na^+]$ increase, measured in the brain by MRI, corresponds to the ischemic core region (Jones et al., 2006). Although MRI detection does not allow discrimination between intracellular and extracellular Na^+ localization, it is plausible to suggest that, in the ischemic core, NCX3, as a result of intracellular Na^+ overload, could be forced to operate in the reverse mode as a Na^+ efflux–Ca^{2+} influx pathway (Amoroso et al., 2000; Annunziato et al., 2004). In accordance with this hypothesis, the electrophysiological data of the present study showed that hypoxia is able to increase the reverse mode of I_{NCX} in ncx3+/+ cortical neurons. More relevantly, in the absence of ncx3 gene, primary cortical neurons, exposed to OGD, displayed a significant reduction in I_{NCX} measured in the reverse mode of operation. Consequently, the present data suggest that NCX3 might have beneficial effects during hypoxic conditions when operating in the reverse mode.

Collectively, the present biochemical and functional data suggest that the fate of neurons in the ischemic core could be in part determined by NCX3. In fact, this isoform, normally expressed in those brain regions (Papa et al., 2003) that belong to the ischemic core, is the only isoform able to preserve its activity despite the occurrence of intense ATP depletion.

Noticeably, the fact that no significant differences were detected in the ischemic brain damage of either ncx3+/− or

ncx3−/− experimental groups could be ascribed to haploinsufficiency, a phenomenon in which the absence of a single functional copy of the gene is able to induce an ischemic phenotype similar to that of knock-out mice.

Overall, based on these results, NCX3 emerges as a new potential molecular target that ought to be further investigated to identify more successful pharmacological interventions against cerebral ischemia.

References

Amoroso S, De Maio M, Russo GM, Catalano A, Bassi A, Montagnani S, Renzo GD, Annunziato L (1997) Pharmacological evidence that the activation of the Na(+)-Ca2+ exchanger protects C6 glioma cells during chemical hypoxia. Br J Pharmacol 121:303–309.

Amoroso S, Tortiglione A, Secondo A, Catalano A, Montagnani S, Di Renzo G, Annunziato L (2000) Sodium nitroprusside prevents chemical hypoxia-induced cell death through iron ions stimulating the activity of the Na+-Ca2+ exchanger in C6 glioma cells. J Neurochem 74:1505–1513.

Annunziato L, Pignataro G, Di Renzo GF (2004) Pharmacology of brain Na+/Ca2+ exchanger: from molecular biology to therapeutic perspectives. Pharmacol Rev 56:633–654.

Bano D, Young KW, Guerin CJ, Lefeuvre R, Rothwell NJ, Naldini L, Rizzuto R, Carafoli E, Nicotera P (2005) Cleavage of the plasma membrane Na+/Ca2+ exchanger in excitotoxicity. Cell 120:275–285.

Boscia F, Annunziato L, Taglialatela M (2006a) Retigabine and flupirtine exert neuroprotective actions in organotypic hippocampal cultures. Neuropharmacology 51:283–294.

Boscia F, Gala R, Pignataro G, de Bartolomeis A, Cicale M, Ambesi-Impiombato A, Di Renzo G, Annunziato L (2006b) Permanent focal brain ischemia induces isoform-dependent changes in the pattern of Na+/Ca2+ exchanger gene expression in the ischemic core, periinfarct area, and intact brain regions. J Cereb Blood Flow Metab 26:502–517.

Gomez-Villafuertes R, Torres B, Barrio J, Savignac M, Gabellini N, Rizzato F, Pintado B, Gutierrez-Adan A, Mellstrom B, Carafoli E, Naranjo JR (2005) Downstream regulatory element antagonist modulator regulates Ca^{2+} homeostasis and viability in cerebellar neurons. J Neurosci 25:10822–10830.

He LP, Cleemann L, Soldatov NM, Morad M (2003) Molecular determinants of cAMP-mediated regulation of the Na+-Ca2+ exchanger expressed in human cell lines. J Physiol (Lond) 548:677–689.

Jones SC, Kharlamov A, Yanovski B, Kim DK, Easley KA, Yushmanov VE, Ziolko SK, Boada FE (2006) Stroke onset time using sodium MRI in rat focal cerebral ischemia. Stroke 37:883–888.

Linck B, Qiu Z, He Z, Tong Q, Hilgemann DW, Philipson KD (1998) Functional comparison of the three isoforms of the Na+/Ca2+ exchanger (NCX1, NCX2, NCX3). Am J Physiol 274:C415–C423.

Longa EZ, Weinstein PR, Carlson S, Cummins R (1989) Reversible middle cerebral artery occlusion without craniectomy in rats. Stroke 20:84–91.

Papa M, Canitano A, Boscia F, Castaldo P, Sellitti S, Porzig H, Taglialatela M, Annunziato L (2003) Differential expression of the Na+-Ca2+ exchanger transcripts and proteins in rat brain regions. J Comp Neurol 461:31–48.

Philipson KD, Nicoll DA (2000) Sodium-calcium exchange: a molecular perspective. Annu Rev Physiol 62:111–133.

Pignataro G, Tortiglione A, Scorziello A, Giaccio L, Secondo A, Severino B, Santagada V, Caliendo G, Amoroso S, Di Renzo G, Annunziato L (2004a) Evidence for a protective role played by the Na+/Ca2+ exchanger in cerebral ischemia induced by middle cerebral artery occlusion in male rats. Neuropharmacology 46:439–448.

Pignataro G, Gala R, Cuomo O, Tortiglione A, Giaccio L, Castaldo P, Sirabella R, Matrone C, Canitano A, Amoroso S, Di Renzo G, Annunziato L (2004b) Two sodium/calcium exchanger gene products, NCX1 and NCX3, play a major role in the development of permanent focal cerebral ischemia. Stroke 35:2566–2570.

Pignataro G, Simon RP, Xiong ZG (2007) Prolonged activation of ASIC1a and the time window for neuroprotection in cerebral ischaemia. Brain 130:151–158.

Scorziello A, Santillo M, Adornetto A, Dell'aversano C, Sirabella R, Damiano S, Canzoniero LM, Renzo GF, Annunziato L (2007) NO-induced neuroprotection in ischemic preconditioning stimulates mitochondrial Mn-SOD activity and expression via RAS/ERK1/2 pathway. J Neurochem 103:1472–1480.

Secondo A, Staiano RI, Scorziello A, Sirabella R, Boscia F, Adornetto A, Valsecchi V, Molinaro P, Canzoniero LM, Di Renzo G, Annunziato L (2007) BHK cells transfected with NCX3 are more resistant to hypoxia followed by reoxygenation than those transfected with NCX1 and NCX2: possible relationship with mitochondrial membrane potential. Cell Calcium 42:521–535.

Sokolow S, Manto M, Gailly P, Molgo J, Vandebrouck C, Vanderwinden JM, Herchuelz A, Schurmans S (2004) Impaired neuromuscular transmission and skeletal muscle fiber necrosis in mice lacking Na/Ca exchanger 3. J Clin Invest 113:265–273.